P1.2 NEAR SURFACE ATMOSPHERIC PLUME DISPERSION THROUGH A COMPACT CYLINDER ARRAY

H. Miner*, M. M. Metzger, J. C. Klewicki, and A. Rasmussen
University of Utah, Salt Lake City, Utah
and
A. Venkatram
University of California, Riverside, California

1. INTRODUCTION

Gas dispersion and plume development in the urban atmosphere has become a topic of increasing importance. With the harmful effects of pollution in cities and threats of biological or chemical warfare, improved characterizations of near surface plumes will be essential to better address these challenges. Given these concerns, detailed experiments of near-field plume dispersion through a uniform array of cylindrical barrels were conducted on the salt flats of Utah's western desert. Results from the study are intended to benefit both the physical understanding of near-field plume behavior in the presence of surface mounted obstacles as well as the development of Lagrangian stochastic models used to predict dispersion in urban environments.

2. EXPERIMENTAL SETUP

To begin to understand the detailed nature of urban plume dispersion, idealized experiments were conducted using a compact 5 $\times$ 9 rectangular array of 45 cylindrical barrels, barrel height $H = 0.91$ m and diameter $d = 0.57$ m, with a barrel spacing of $2H$, center to center. Figure 1 depicts a scaled drawing of the experimental grid setup where each of the grid intersections represents a barrel. For clarity, the center barrel, just downwind of the source, is drawn to scale in the grid. Propylene tracer gas was released through a 25.4 mm diameter pipe within the barrel array as shown in the experimental grid setup. The dissemination rate was fixed at 15 slm using a precision mass flow controller.

The tracer source was located at both ground level and $1H$. At each of the two source heights, four different barrel configurations were arranged near the source. In the first and second configurations, the source was located directly upwind of a single barrel and two barrels placed side by side, respectively. In the third configuration four barrels surrounded the source. In the final configuration the source was located upwind of a three-barrel pyramid. Instantaneous concentration measurements were simultaneously acquired within the array from 40 digital photo-ionization detectors (digiPID, Aurora Scientific) that were arranged in three, 50 degree arcs, also depicted in figure 1. As displayed in the grid setup, the arcs were placed at three different radii of $R = 3H$, $5H$, $9H$, relative to the source location. Five degrees separated each sensor on each arc. Most of the sensors were placed at ground level ($0.25H$); however a limited set of sensors were placed on towers at $0.25H$, $0.5H$, and $1.5H$. Turbulence data in the roughness sub layer and near the source were also acquired using 3–6, three-dimensional sonic anemometers.

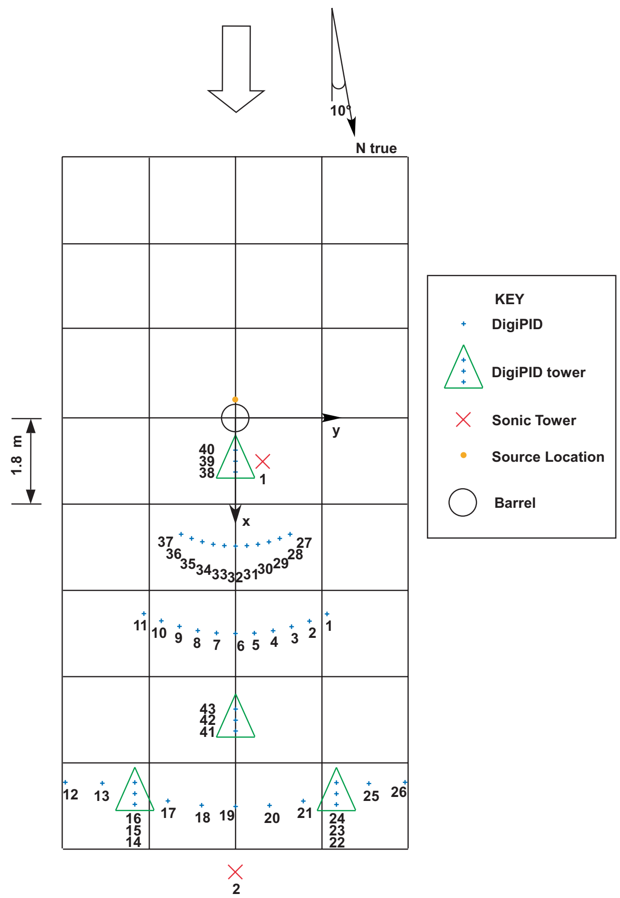

Figure 1. Scaled drawing of the experimental grid setup.

3. RESULTS

Overall, 13.5 hours of velocity and concentration time

*Corresponding author address: Heidi Miner, Dept. of Mechanical Engineering, 2202 MEB, University of Utah, Salt Lake City, UT 84112; email: heidi.miner@utah.edu

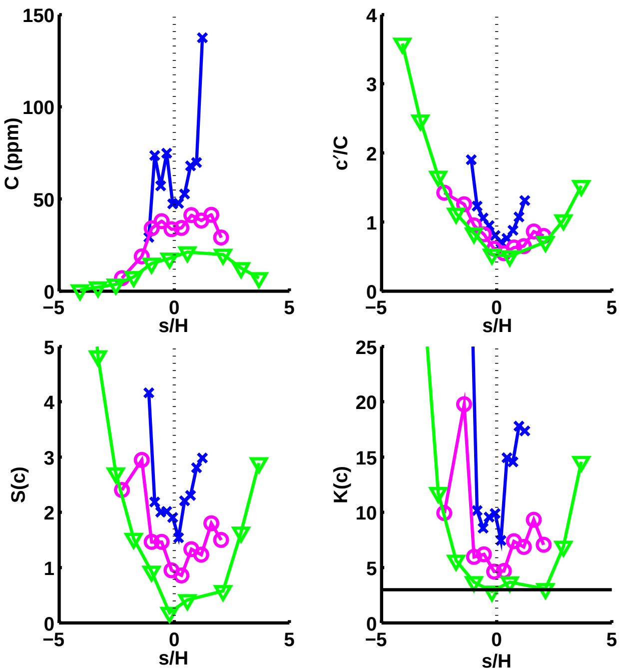

Figure 2. Statistical profiles of c as a function of arc length, $z/H = 0.25$. $\times$, $R/H = 3$; $\bigcirc$, $R/H = 5$; $\triangledown$, $R/H = 9$.

series measurements were obtained within the barrel array. Atmospheric stability during the experiments ranged between -0.8 $< \zeta <$ 0.4, where ζ denotes the Monin-Obukhov stability parameter as calculated from a sonic anemometer located at a height of $3.5H$. Statistical profiles of the concentration c as a function of arc length, normalized by barrel height, for a neutrally stable case (-0.1 $< \zeta <$ 0.1) are presented in figure 2. The jagged appearance in the mean profile at $R/H = 3$ may be due to an effect of vortex shedding, as based upon a preliminary comparison of spectra and rough calculations of the expected vortex shedding frequency.

Along the plume centerline, skewness and kurtosis values approach zero and three, respectively, with downwind distance from the source, thereby indicating a relaxation to Gaussain behavior. This is also visible in the probability density functions (PDFs), as shown in the histograms of figure 3. The corresponding time series for each of the three PDFs are plotted in figure 4. In presenting these results, however, it needs to be stated that stability plays an important role in determining the rate at which centerline plume statistics relax to Gaussian behavior with downwind distance from the source. For example, in the unstable case (-0.5 $< \zeta <$ -0.1), skewness and kurtosis values along the plume centerline ranged from 0.5–1, and 3–5, respectively, at $R/H = 9$, thus Gaussian behavior was not attained at this location. These results appear to be independent of source configuration. Data from an unroughened sublayer, with the barrels absent, demonstrated a much slower relaxation to Gaussian behavior along the plume centerline. In this case, the skewness and kurtosis values under neutrally stable condidions, were approximately 1.3 and 4, respectively at $R/H = 17.6$, almost twice as far downstream as any data acquired in the barrel array.

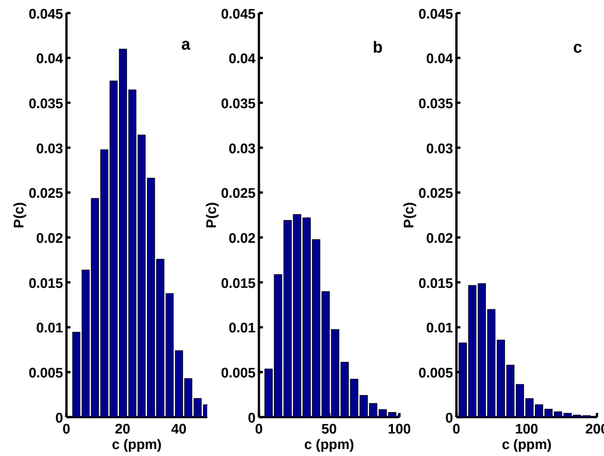

Figure 3. Probability histograms of c for the three sensors located along the plume centerline, $z/H = 0.25$. (a)$R/H = 9$, (b)$R/H = 5$, and (c)$R/H = 3$.

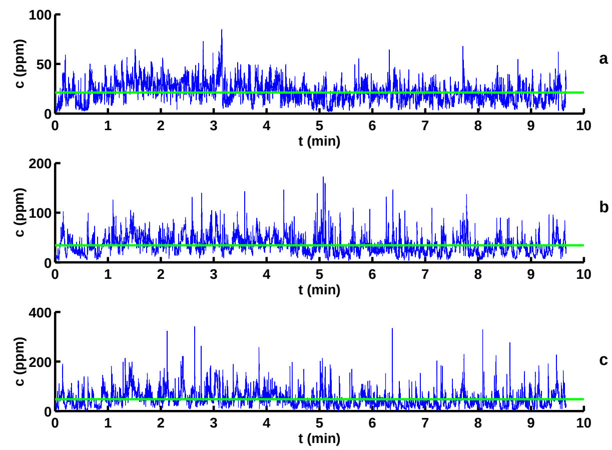

Figure 4. Time series of c corresponding to the three PDFs in figure 3, $z/H = 0.25$. (a)$R/H = 9$, (b)$R/H = 5$, and (c)$R/H = 3$. The grey lines denote the mean value of the record.

4. ACKNOWLEDGEMENTS

This work was supported by a contract with the California Air Resources Board, Sacramento, California, contract number 99–319. The authors would also like to acknowledge the help of Chris Biltoft, U.S. Army Dugway Proving Ground, during the field trials.